A&A 402, L63–L67 (2003)
DOI: 10.1051/0004-6361:20030341

Astronomy & Astrophysics

Letter to the Editor

Odin observations of H_2O in the Galactic Centre⋆

Aa. Sandqvist[1], P. Bergman[2], J. H. Black[2], R. Booth[2], V. Buat[3], C. L. Curry[4], P. Encrenaz[5], E. Falgarone[6], P. Feldman[7], M. Fich[4], H. G. Floren[1], U. Frisk[8], M. Gerin[6], E. M. Gregersen[9], J. Harju[10], T. Hasegawa[11], Å. Hjalmarson[2], L. E. B. Johansson[2], S. Kwok[11], B. Larsson[1], A. Lecacheux[12], T. Liljeström[13], M. Lindqvist[2], R. Liseau[1], K. Mattila[10], G. F. Mitchell[14], L. Nordh[15], M. Olberg[2], A. O. H. Olofsson[2], G. Olofsson[1], L. Pagani[5], R. Plume[11], I. Ristorcelli[16], F. v. Schéele[8], G. Serra[16], N. F. H. Tothill[14], K. Volk[11], C. D. Wilson[9], and A. Winnberg[2]

1 Stockholm Observatory, SCFAB-AlbaNova, 106 91 Stockholm, Sweden
2 Onsala Space Observatory, 439 92 Onsala, Sweden
3 Laboratoire d'Astronomie Spatiale, BP 8, 13376 Marseille Cedex 12, France
4 Department of Physics, University of Waterloo, Waterloo, ON N2L 3G1, Canada
5 LERMA & FRE 2460 du CNRS, Observatoire de Paris, 61 Av. de l'Observatoire, 75014 Paris, France
6 LERMA & FRE 2460 du CNRS, École Normale Supérieure, 24 rue Lhomond, 75005 Paris, France
7 Herzberg Institute of Astrophysics, 5071 West Saanich Road, Victoria, BC V9E 2E7, Canada
8 Swedish Space Corporation, PO Box 4207, 171 04 Solna, Sweden
9 Department of Physics and Astronomy, McMaster University, Hamilton, ON L8S 4M1, Canada
10 Observatory, PO Box 14, University of Helsinki, 00014 Helsinki, Finland
11 Department of Physics and Astronomy, University of Calgary, Calgary, AB T2N 1N4, Canada
12 LESIA, Observatoire de Paris, Section de Meudon, 5 place Jules Janssen, 92195 Meudon Cedex, France
13 Metsähovi Radio Observatory, Helsinki University of Technology, Otakaari 5A, 02150 Espoo, Finland
14 Department of Astronomy and Physics, Saint Mary's University, Halifax, NS B3H 3C3, Canada
15 Swedish National Space Board, Box 4006, 171 04 Solna, Sweden
16 CESR, 9 avenue du Colonel Roche, BP 4346, 31029 Toulouse, France

Received 2 December 2002 / Accepted 11 February 2003

Abstract. The Odin satellite has been used to detect emission and absorption in the 557-GHz $H_2^{16}O$ line in the Galactic Centre towards the Sgr A⋆ Circumnuclear Disk (CND), and the Sgr A +20 $km\,s^{-1}$ and +50 $km\,s^{-1}$ molecular clouds. Strong broad H_2O emission lines have been detected in all three objects. Narrow H_2O absorption lines are present at all three positions and originate along the lines of sight in the 3-kpc Spiral Arm, the −30 $km\,s^{-1}$ Spiral Arm and the Local Sgr Spiral Arm. Broad H_2O absorption lines near −130 $km\,s^{-1}$ are also observed, originating in the Expanding Molecular Ring. A new molecular feature (the "High Positive Velocity Gas" - HPVG) has been identified in the positive velocity range of ≈+120 to +220 $km\,s^{-1}$, seen definitely in absorption against the stronger dust continuum emission from the +20 $km\,s^{-1}$ and +50 $km\,s^{-1}$ clouds and possibly in emission towards the position of Sgr A⋆ CND. The 548-GHz $H_2^{18}O$ isotope line towards the CND is not detected at the 0.02 K (rms) level.

Key words. Galaxy: center – ISM: individual objects: Sgr A – ISM: molecules – ISM: clouds

1. Introduction

The central region of the Galaxy has been extensively studied at wavelengths between the near infrared and the radio portions of the spectrum (see reviews by Morris & Serabyn 1996; Mezger et al. 1996) as well as at γ-ray and X-ray wavelengths. The molecular clouds dominate the interstellar medium in the inner 500 pc (1° = 150 pc) of the Galaxy and the density of molecular clouds is far higher in this region than in any other part of the Galaxy. Although it represents less than 0.2% of the Galactic disk by volume, nearly 10% of the total Galactic molecular mass is found here. A dominant feature in this region is the inclined Expanding Molecular Ring (EMR, e.g. Güsten 1989). Another feature closer to the Centre is Sgr B2 which is the most prominent and massive concentration of molecular gas (GMC) and star formation in the entire Galaxy. Neufeld et al. (2000) have observed both $H_2^{16}O$ and $H_2^{18}O$ towards this source using the Submillimetre Wave Astronomy Satellite (SWAS). A dust ridge connects Sgr B2 to the regions closer to the Centre (Lis & Carlstrom 1994). The very central Sgr A Complex consists of a nonthermal shell component, Sgr A East, and a thermal

Send offprint requests to: Aa. Sandqvist, e-mail: aage@astro.su.se
⋆ Based on observations with Odin, a Swedish-led satellite project funded jointly by the Swedish National Space Board (SNSB), the Canadian Space Agency (CSA), the National Technology Agency of Finland (Tekes) and Centre National d'Études Spatiales (CNES). The Swedish Space Corporation was the industrial prime contractor and is also responsible for the satellite operation.

component, Sgr A West. The source Sgr A West, with its "mini-spiral arms", consists of infalling gas (Killeen & Lo 1989) and contains in its innermost regions the unique nonthermal radio source Sgr A*, which is the manifestation of a 2.6×10^6 $M_\odot$ black hole in the centre of the Milky Way system (Eckart & Genzel 1996; Schödel et al. 2002).

The molecular complex associated with Sgr A consists predominantly of a molecular belt comprising the "+50 km s^{-1} cloud" (M–0.02–0.07), the "+20 km s^{-1} cloud" (M–0.13–0.08), and the Circumnuclear Disk (CND) which surrounds Sgr A West and has a rotational velocity of the order of 100 km s^{-1} in the same direction as the rotation of the Galaxy. These warm and high-density Galactic Centre molecular clouds are intimately entwined and interact with the continuum complex described above (Sandqvist 1989 – H_2CO; Zylka et al. 1990, 1996; Serabyn et al. 1994; Ojha et al. 2001 – C I; Lindqvist et al. 1995 – $C^{18}O$, HNCO; Pak et al. 1996 – H_2). All these structures, together with many more, are parts of a mechanism complex involving shocks, magnetic fields and strong UV radiation fields, and may thus function as prime candidates for H_2O observations with the Odin satellite.

2. Observations

Odin is a submillimetre/millimetre wave spectroscopy astronomy and aeronomy satellite, launched on 20 February 2001 from Svobodny, Russia in far-eastern Siberia. It has a 1.1-m high-precision telescope with a beam efficiency of about 90% and beamwidths of $2'.1$ and $9'.5$ at submm and mm wavelengths, respectively. Its pointing uncertainty is $<10''$. There are four cryo-cooled submm receivers tunable in the frequency range of 486–580 GHz with a single sideband temperature of ≈3000 K. A cryo-cooled HEMT receiver is tuned to 119 GHz and has a single sideband temperature of ≈600 K. The backend spectrometers consist of an acousto-optical spectrometer (AOS) with a total bandwidth of 1040 MHz and two auto-correlators with bandwiths in the range of 100–800 MHz, corresponding to velocity resolutions of 0.08–1.0 km s^{-1}. The satellite is described in detail by Frisk et al. (2003) and the receiver calibration by Olberg et al. (2003).

Three positions towards Sgr A have so far been observed with Odin, namely Sgr A* with the CND, the +20 km s^{-1} molecular cloud and the +50 km s^{-1} molecular cloud. The coordinates of the observed positions are given in Table 1. Observations have been made in the spectral lines of 119-GHz O_2, 487-GHz O_2, 492-GHz C I, 548-GHz $H_2^{18}O$, 557-GHz $H_2^{16}O$, and 576-GHz ($J = 5 - 4$) CO. However, only the data for $H_2^{16}O$ and $H_2^{18}O$ have been fully calibrated and reduced so far and they are presented in Sect. 3. The data for the other spectral lines will be presented in a subsequent paper.

Two observing methods have been employed with Odin. One method is Dicke-switching against one of two sky horns with beamwidths of $4^\circ.4$, displaced 42° from the main beam. Sgr A* CND was observed this way in the $H_2^{16}O$ line during October 2001. In order to improve the baselines, full-orbit observations were made of an empty reference OFF-position at $\alpha(1950.0) = 17^h40^m26^s.8$, $\delta(1950.0) = -28°35'04''$ every second orbit (observing period of 60 min). The total ON-position time for the $H_2^{16}O$ line observations was eight orbits (480 min). The other observing method was total-power position-switching to the above reference position with a duty cycle of 120 s. This was used for $H_2^{16}O$ observations of the +20 km s^{-1} (18 orbits) and the +50 km s^{-1} (27 orbits) clouds and for $H_2^{18}O$ observations of the Sgr A* CND-region (58 orbits) during April/May 2002. The AOS was used for all the H_2O observations, which results in a velocity resolution of 0.54 km s^{-1} and a total velocity coverage of 560 km s^{-1} in the line profiles.

Table 1. Observed positions in the Galactic Centre Sgr A region.

	$\alpha(1950.0)$	$\delta(1950.0)$
Sgr A* Circumnuclear Disk	$17^h42^m29^s.3$	$-28°59'18''$
Sgr A +20 km s^{-1} cloud	$17^h42^m29^s.3$	$-29°02'18''$
Sgr A +50 km s^{-1} cloud	$17^h42^m41^s.0$	$-28°58'00''$

3. Results

Strong emission and absorption lines have been observed in the $H_2^{16}O$ line at all three Sgr A positions. However, no spectral line features can be detected in the $H_2^{18}O$ line down to the rms noise limit of ≈0.02 K. The three 557-GHz $H_2^{16}O$ line profiles observed towards Sgr A* CND, the +20 km s^{-1} cloud and the +50 km s^{-1} cloud, are presented in Figs. 1a–c, and the smooth featureless (<0.02 K rms) profile of the 548-GHz $H_2^{18}O$ line towards Sgr A* CND is shown in Fig. 1d. This last profile gives an indication of the high quality of the baselines in our broadband observations, which is important when judging the reality of the many emission and absorption features in the $H_2^{16}O$ profiles. The intensity scale has not been corrected for the main beam efficiency (≈0.9) in these four profiles. Furthermore, no baselines have been subtracted. The intensity thus includes the presence of the background continuum emission, although the uncertainty of this level is not yet determined. The relative continuum intensities for the $H_2^{16}O$ observations conform qualitatively to the continuum level expected from an interpolation to the H_2O frequency of the 800 and 350 μm maps by Lis & Carlstrom (1994) and Dowell et al. (1999), respectively. However, it seems that the continuum level obtained with the Dicke-switching method (Fig. 1a) agrees better with the interpolated results (see also Sect. 4) than the position-switching method (Figs. 1b–d). For the sake of comparison with other spectral lines, we have chosen the data from the SEST $C^{18}O$ (1 – 0) survey of the Galactic Centre by Lindqvist et al. (1995). The $C^{18}O$ profiles resulting for the three H_2O positions from a convolution of the SEST map spectra to a resolution of 2′ (corresponding to the Odin beam size) are shown in Fig. 2.

4. Discussion

A Gaussian analysis has been performed on the Sgr A* CND $H_2^{16}O$ profile using four absorption components and two emission components (Fig. 3). The continuum emission was first

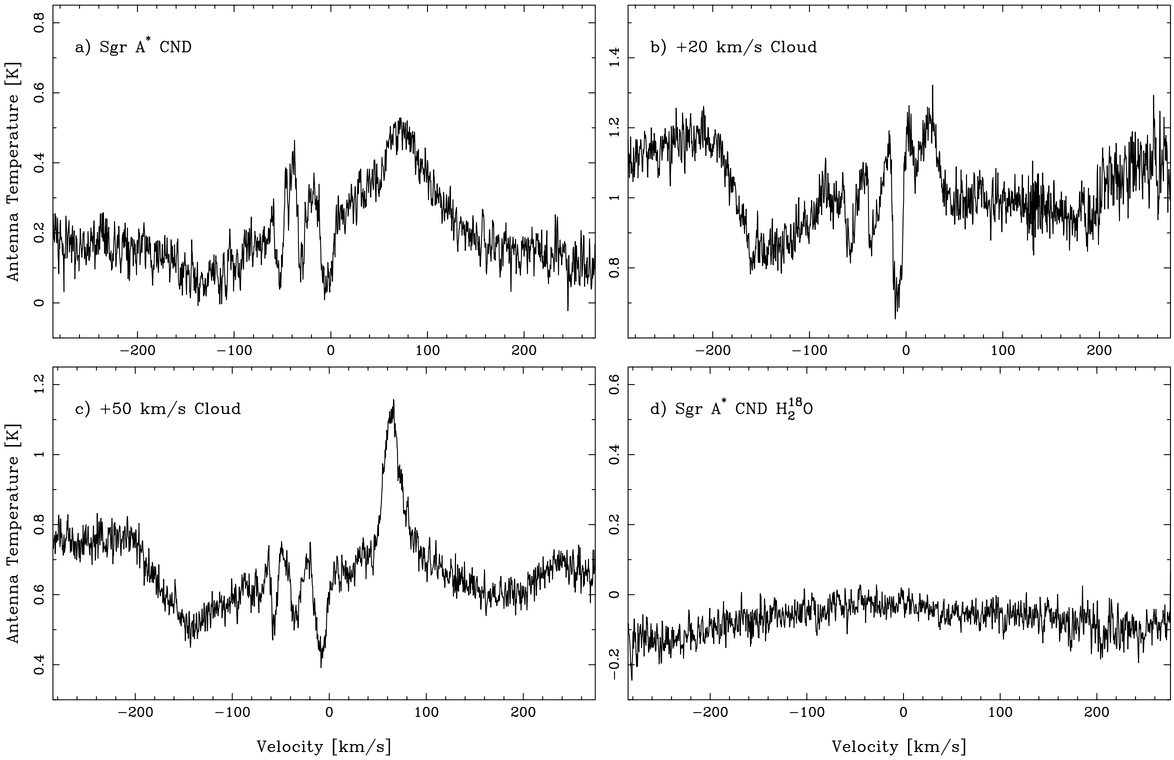

Fig. 1. The 557-GHz $H_2^{16}O$ line profiles observed towards **a)** the Sgr A⋆ Circumnuclear Disk, the **b)** +20 and **c)** +50 $km\,s^{-1}$ clouds, and **d)** the 548-GHz $H_2^{18}O$ isotope line profile observed towards the Sgr A⋆ Circumnuclear Disk.

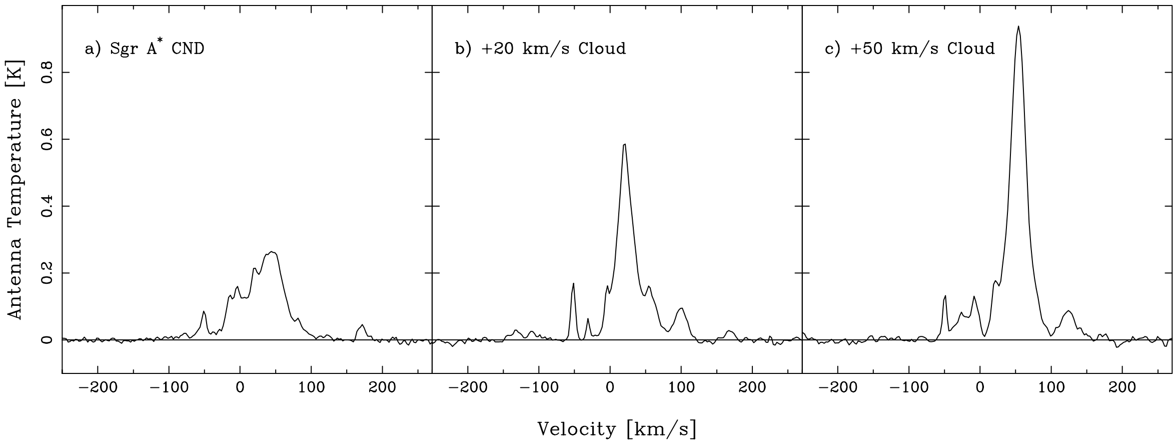

Fig. 2. The SEST $C^{18}O$ (1–0) survey Odin-beam convolved profiles towards **a)** the Sgr A⋆ Circumnuclear Disk, the **b)** +20 and **c)** +50 $km\,s^{-1}$ clouds.

subtracted out by fitting a linear baseline to the outermost channels on either side of the profile. The Gaussian analysis results are given in Table 2.

The first two components, I and II, both seen in emission, are believed to originate in the rapidly rotating CND. The northeastern part of the CND is receding and the southwestern part approaching, which gives the asymmetric, somewhat double-peaked line profile structure. The 2.1-arcmin beam of Odin encloses fully the CND and the resulting velocity structure of the profile is reminiscent of that seen in many other molecular lines (see e.g. HCO^+ (1 − 0) – Linke et al. 1981; HCO^+ (3 – 2) – Sandqvist et al. 1985; H_2CO (2 – 1) and CS (5 – 4) – Sandqvist 1989; CO (4 – 3) – White 1996).

Three narrow H_2O absorption components, seen at velocities near –5, –30 and –53 $km\,s^{-1}$, are observed at all three positions and are well-known Galactic spiral arm features, which were first identified in early 21-cm H I observations. They originate along the line of sight crossing the so-called Local Sgr, –30 $km\,s^{-1}$ and 3-kpc spiral arm structures.

From the two submillimetre continuum maps discussed in Sect. 3, we find that the 350 μm:800 μm flux ratios (on a 30″ scale) for all three positions are about 17–18 (corresponding to a spectral index of about 3.5). From the 800 μm map we estimate the flux densities on a 2′ scale to be 160, 300, and 250 Jy, for the Sgr A⋆ CND, +20 and +50 $km\,s^{-1}$ cloud positions, respectively. At 557 GHz

Table 2. Gaussian components of the Sgr A⋆ Circumnuclear Disk 557-GHz $H_2^{16}O$ line profile.

	Velocity ($km\,s^{-1}$)	T_A^* (K)	Halfwidth ($km\,s^{-1}$)	Source
I	+73.2	+0.32	88.5	CND
II	−31.6	+0.24	47.9	CND
III	−4.8	−0.24	13.4	Local Sgr Arm
IV	−30.2	−0.25	11.0	−30 $km\,s^{-1}$ Arm
V	−53.5	−0.21	8.1	3-kpc Arm
VI	−132.2	−0.09	60.0	EMR

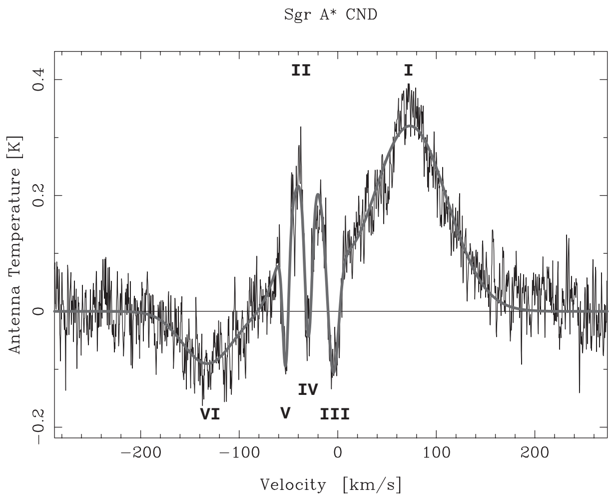

Fig. 3. Gaussian analysis performed on the 557-GHz $H_2^{16}O$ line profile observed towards the Sgr A⋆ Circumnuclear Disk.

(538 μm) and with a conversion factor of 4100 Jy/K (based on a theoretical $\eta_a = 0.7$ for Odin) we estimate continuum levels of 0.16, 0.29, and 0.24 K in our three positions. In the +20 $km\,s^{-1}$ cloud profile the deepest absorption is about 0.4 K which is significantly deeper than our estimated continuum level of 0.29 K.

The three distinct and rather narrow absorption features (III, IV and V) are present in the spectra at all three positions (see Figs. 1a–c). The absorption feature (III) at –5 $km\,s^{-1}$ appears to be the strongest and, judged by the estimated continuum levels, this feature has an optical depth of at least one. The absorbing gas in these three features lies in front of the thermal (and non-thermal) continuum sources as well as H_2O gas seen in emission. Since it is not known how the foreground gas is distributed with respect to the continuum sources and the H_2O gas seen in emission and since our estimates of the continuum levels are uncertain, we shall refrain from calculating the optical depths of the absorption features. However, when estimating the (lower) limits of the water column density we shall assume that the optical depths are ≥1.

We can estimate the H_2 column densities using the $C^{18}O$-profiles in Fig. 2 and calculating the integrated intensities over the regions corresponding to the three narrow H_2O absorptions. The H_2 column densities have been calculated by assuming optically thin emission, an excitation temperature of 15 K and a $C^{18}O$ abundance of 2×10^{-7} with respect to H_2 (Frerking et al. 1982). The lower H_2O column density limits, using the appropriate line width for each absorption feature and an excitation temperature of 15 K, have been calculated from the assumption that the optical depths are ≥1. The corresponding H_2O abundance limits are then obtained by using the H_2 column density estimates from the $C^{18}O$ data. The results are summarized in Table 3.

A broad H_2O absoption component (VI), seen at velocities near –132 $km\,s^{-1}$, is also observed in all three positions. This feature has its origin in the near side of the Expanding Molecular Ring (EMR). The EMR is a massive ≈180 pc molecular ring surrounding the Galactic Centre and it has been observed in many atomic and molecular species (e.g. Morris & Serabyn 1996). The near side is seen in broad absorption lines towards the Sgr A Complex at velocities of ≈–130 $km\,s^{-1}$, while the far side is seen only in emission lines, which towards the Sgr A Complex have velocities near +170 $km\,s^{-1}$.

Now let us turn our attention to the H_2O profiles observed towards the +20 and +50 $km\,s^{-1}$ clouds, presented in Figs. 1b, c. In addition to the four absorption features discussed above, the profiles are marked by the characteristic emission component from these molecular clouds at velocities near +20 $km\,s^{-1}$ and +50 $km\,s^{-1}$, respectively. Furthermore, a new molecular feature in the Galactic Centre can now been identified. It is detected as broad $H_2^{16}O$ absorption in the velocity range of ≈+120 to +220 $km\,s^{-1}$ (see Figs. 1b, c). We shall call this feature the High Positive Velocity Gas (HPVG). This feature is not seen in the Sgr A⋆ CND profile (Fig. 1a), which we interpret as being due to the background continuum emission seen at this position being somewhat lower than towards the dust continuum peak emission from the Sgr A +20 and +50 $km\,s^{-1}$ molecular clouds (see the 800 and 350 μm continuum maps of Lis & Carlstrom 1994 and Dowell et al. 1999, respectively). However, a careful study of the H_2O profile in Fig. 1a (and Fig. 3) may show an extended very weak emission wing in this HPVG velocity range, so there may be still HPVG present even towards the Sgr A⋆ CND region, although here the background continuum is too weak to cause visible absorption. Alternatively, the high positive velocity wing of the CND emission may mask any HPVG absorption.

Evidence for the existence of the HPVG in the Sgr A region, seen in other spectral lines, is scarce. The HPVG should not be confused with the molecular gas in the far side of the EMR whose velocity falls inside the same range but whose emission lines are narrower. Also, the HPVG is seen in absorption which places it in front of the Galactic Centre continuum sources and thus it cannot be part of the far side of the EMR. Moneti et al. (2001) have used the Infrared Space Observatory (ISO) to obtain mid- and far-infrared H_2O profiles towards Sgr A. These profiles do indeed show some absorption components at velocities corresponding to that of the HPVG. Some evidence for the HPVG may also be present in VLA OH absorption observations towards the Sgr A Complex by Karlsson et al. (2003).

Additional evidence for the HPVG is also apparent in the data of a new high-resolution H I absorption survey of the Galactic Centre region performed with the VLA by Dwarakanath et al. (2003, in preparation). They have kindly

Table 3. Abundances in the Local Sgr (III), –30 km s^{-1} (IV) and 3-kpc (V) Spiral Arm features.

Position	Feature	$I(C^{18}O)$ (K km s^{-1})	$N(C^{18}O)$ (cm^{-2})	$N(H_2)$ (cm^{-2})	$N[H_2O]$ (cm^{-2})	X [H_2O]
Sgr A* CND	III	2.10	2.1×10^{15}	1.0×10^{22}	$>2 \times 10^{13}$	$>2 \times 10^{-9}$
	IV	0.18	1.8×10^{14}	9.0×10^{20}	$>9 \times 10^{12}$	$>1 \times 10^{-8}$
	V	0.65	6.5×10^{14}	3.2×10^{21}	$>8 \times 10^{12}$	$>2 \times 10^{-9}$
+20 km s^{-1} cloud	III	1.00	1.0×10^{15}	5.0×10^{21}	$>1 \times 10^{13}$	$>2 \times 10^{-9}$
	IV	0.34	3.4×10^{14}	1.7×10^{21}	$>1 \times 10^{13}$	$>6 \times 10^{-9}$
	V	0.96	9.6×10^{14}	4.8×10^{21}	$>2 \times 10^{13}$	$>4 \times 10^{-9}$
+50 km s^{-1} cloud	III	1.10	1.1×10^{15}	5.5×10^{21}	$>2 \times 10^{13}$	$>4 \times 10^{-9}$
	IV	0.64	6.4×10^{14}	3.2×10^{21}	$>1 \times 10^{13}$	$>3 \times 10^{-9}$
	V	0.81	8.1×10^{14}	4.0×10^{21}	$>6 \times 10^{12}$	$>2 \times 10^{-9}$

convolved their data with the Odin beam at our positions and find that (1) towards the +20 km s^{-1} cloud there is an H I absorption with an optical depth of ∼0.03 at +100 km s^{-1}, decreasing to ∼0 around +130 km s^{-1} and a second absorption component centred around +150 km s^{-1} with an optical depth of ∼0.03 and a width of ∼20 km s^{-1}, and (2) towards the +50 km s^{-1} cloud in the velocity range of +100 to +200 km s^{-1} there is an H I absorption with the optical depth decreasing monotonically from ∼0.04 at +100 km s^{-1} to ∼0 at +200 km s^{-1}.

Although 58 Odin orbits were dedicated to observing the $H_2^{18}O$ line towards the Sgr A* CND position, no spectral line was detected (see Fig. 1d). Our non-detection of $H_2^{18}O$ towards Sgr A* CND provides an upper limit on the H_2O abundance in the narrow absorption features. Given the rms noise of 23 mK in the $H_2^{18}O$ spectrum and the estimated continuum level of 0.16 K we find that a 10 km s^{-1} wide absorption feature of optical depth 0.08 should have been detected at the 3σ level. Using this limit and adopting a $^{16}O/^{18}O$ ratio of 500 for this local absorbing cloud (Wilson & Rood 1994) and an excitation temperature of 15 K, we obtain an H_2O column density of 5×10^{14} cm^{-2}. Hence, for the Local Sgr Arm absorption, the 3σ upper limit of the H_2O abundance becomes 5×10^{-8}, using the H_2 column density of 1.0×10^{22} in Table 3, while the lower limit was found to be 2×10^{-9}. The average H_2O abundance estimated for the foreground gas towards Sgr B2 by Neufeld et al. (2000) is 6×10^{-7}, which is about an order of magnitude higher than our range towards Sgr A. On the other hand, our range is in better agreement with H_2O abundances found in giant molecular cloud cores by Snell et al. (2000) and in a local diffuse molecular cloud by Neufeld et al. (2002).

In September/October of 2002, Odin again observed the Galactic Centre region in the $H_2^{18}O$ line, this time pointing at the +20 and +50 km s^{-1} cloud positions. These observations have not yet been calibrated and reduced. They will be reported in a future paper.

Acknowledgements. We should like to thank K. Dwarakanath, J.-H. Zhao, M. Goss and C. Lang for permission to use some of their VLA Sgr A Complex H I absorption line results before publication and K. Dwarakanath for making the Odin-compatible analysis of their H I data.

References

Dowell, C. D., Lis, D. C., Serabyn, E., et al. 1999, SHARC 350 μm Mapping of the Galactic Center from the Caltech Submillimetr Observatory, in The Central Parsec of the Galaxy, ed. H. Falcke, W. J. Cotera, W. J. Duschl, F. Melia, & M. J. Rieke, ASP Conf. Ser., 186, 453
Eckart, A., & Genzel, R. 1996, Nature, 383, 415
Frerking, M. A., Langer, W. D., & Wilson, R. W. 1982, ApJ, 262, 590
Frisk, U., Hagström, M., Ala-Laurinaho, J., et al. 2003, A&A, 402, L27
Güsten, R. 1989, in Gas and Dust in the Inner Few Degrees of the Galaxy, The Center of the Galaxy, ed. M. Morris (Dordrecht: Kluwer), IAU Symp., 136, 89
Karlsson, R., Sjouwerman, L. O., Sandqvist, Aa., & Whiteoak, J. B. 2003, A&A, in press
Killeen, N. E. B., & Lo, K. Y. 1989, in High Quality VLA Imaging of Sgr A West at 6 cm, The Center of the Galaxy, ed. M. Morris (Dordrecht: Kluwer), IAU Symp., 136, 453
Lindqvist, M., Sandqvist, Aa., Winnberg, A., Johansson, L. E. B., & Nyman, L-Å. 1995, A&AS, 113, 257
Linke, R., Stark, A. A., & Frerking, M. A. 1981, ApJ, 243, 147
Lis, D. C., & Carlstrom, J. E. 1994, ApJ, 424, 189
Mezger, P. G., Duschl, W. J., & Zylka, R. 1996, A&AR, 4, 289
Moneti, A., Cernicharo, J., & Pardo, J. R. 2001, ApJ, 549, L203
Morris, M., & Serabyn, E. 1996, ARA&A, 34, 645
Neufeld, D. A., Ashby, M. L. N., Bergin, G., et al. 2000, ApJ, 539, L111
Neufeld, D. A., Kaufman, M. J., Goldsmith, P. F., Hollenbach, D. J., & Plume, R. 2002, ApJ, 580, 278
Ojha, R., Stark, A. A., Hsieh, H. H., et al. 2001, ApJ, 548, 253
Olberg, M., Frisk, U., Lecacheux, A., et al. 2003, A&A, 402, L35
Pak, S., Jaffe, D. T., & Keller, L. D. 1996, ApJ, 457, L43
Sandqvist, Aa. 1989, A&A, 223, 293
Sandqvist, Aa., Wootten, A., & Loren, R. B. 1985, A&A, 152, L25
Schödel, R., Ott, T., Genzel, R., et al. 2002, Nature, 419, 694
Serabyn, E., Keene, J., Lis, D. C., & Phillips, T. G. 1994, ApJ, 424, L95
Snell, R. L., Howe, J. E., Ashby, M. L. N., et al. 2000, ApJ, 539, L101
White, G. 1996, Molecular Line Maps of the Galactic Centre Circumnuclear Disc, in The Galactic Center, 4th ESO/CTIO Workshop, ed. R. Gredel, ASP Conf. Ser., 102, 171
Wilson, T. L., & Rood, R. 1994, ARA&A, 32, 191
Zylka, R. 1996, Kinematics of the Sgr A Cloud Complex, The Galactic Center, 4th ESO/CTIO Workshop, ed. R. Gredel, in ASP Conf. Ser., 102, 77
Zylka, R., Mezger, P. G., & Wink, J. E. 1990, A&A, 234, 133